SCIENCE CHINA
Life Sciences

• RESEARCH PAPER •

November 2012 Vol.55 No.11: 958–967
doi: 10.1007/s11427-012-4400-1

A simulation study on the relation between muscle motor unit numbers and the non-Gaussianity/non-linearity levels of surface electromyography

ZHAO Yan[1,2*] & LI DongXu[1,2]

[1]*College of Aerospace Science and Engineering, National University of Defense Technology, Changsha 410073, China;*
[2]*Science and Technology on Human Factors Engineering Laboratory, China Astronaut Research and Training Center, Beijing 100094, China*

Received August 10, 2012; accepted October 16, 2012

Recent research has demonstrated that surface electromyography (sEMG) signals have non-Gaussianity and non-linearity properties. It is known that more muscle motor units are recruited and firing rates (FRs) increase as exertion increases. A hypothesis was proposed that the Gaussianity test (S_g) and linearity test (S_ℓ) levels of sEMG signals are associated with the number of active motor units (nMUs) and the FR. The hypothesis has only been preliminarily discussed in experimental studies. We used a simulation sEMG model involving spatial (active MUs) and temporal (three FRs) information to test the hypothesis. Higher-order statistics (HOS) from the bi-frequency domain were used to perform S_g and S_ℓ. Multivariate covariance analysis and a correlation test were employed to determine the nMUs-S_g relationship and the nMUs-S_ℓ relationship. Results showed that nMUs, the FR, and the interaction of nMUs and the FR all influenced the S_g and S_ℓ values. The nMUs negatively correlated to both the S_g and S_ℓ values. That is, at the three FRs, sEMG signals tended to a more Gaussian and linear distribution as exertion and nMUs increased. The study limited experiment factors to the sEMG non-Gaussianity and non-linearity levels. The study quantitatively described nMUs and the FR of muscle that are not directly available from experiments. Our finding has guiding significance for muscle capability assessment and prosthetic control.

simulation surface electromyography model, higher-order statistics, motor unit, firing rate

Citation: Zhao Y, Li D X. A simulation study on the relation between muscle motor unit numbers and the non-Gaussianity/non-linearity levels of surface electromyography. Sci China Life Sci, 2012, 55: 958−967, doi: 10.1007/s11427-012-4400-1

A motor unit (MU) consists of an alpha motor neuron and connected muscle fibers [1]. An MU structure is made up of a motor neuron, an axon, muscle fibers and a motor endplate [2]. When an MU fires, an action potential is carried down the motor neuron to the muscle. The location where the nerve contacts the muscle is called the motor endplate. After an action potential is transmitted across the motor endplate, an action potential is elicited in all of the innervational muscle fibers of that particular MU. The potential distribution generated in the volume conductor surrounding the fibers of each MU is referred to as "motor unit action potential" (MUAP) [3]. The surface electromyography (sEMG) signal is an algebraic summation of MUAPs [4].

In past research, sEMG signals were usually assumed to be Gaussian with zero mean. However, recent research has indicated that sEMG signals have non-Gaussian and non-linear properties [2,5,6]. Higher-order statistics (HOS) from the bi-frequency domain are able to recover more information from non-Gaussian and non-linear signals via their higher-order moments, cumulants, and spectral representations, and they do not suppress the phase relationship [7]. The HOS approach was recently used to analyze non-Gaussianity and non-linearity sEMG [8]. In specific examples, Bilodeau *et al*. [5] examined biceps brachii (BB)

*Corresponding author (email: yanzhao@nudt.edu.cn)

and brachioradialis step and ramp contractions. For the step contractions, four force levels (20%, 40%, 60% and 80% maximum voluntary contraction (MVC)) were maintained for a period of 3 s each. Ramp contractions were performed from 0% to 100% of MVC in a 5-s period. It was found that the amplitude distributions of both BB and brachioradialis sEMG signals were non-Gaussian, and higher forces gave rise to a slightly more normal sEMG distribution. Applying step contraction tests for a period of 5 s, Nazrpour *et al*. [9] demonstrated that the non-Gaussianity of BB sEMG signals below 25% of MVC was significant. Kaplanis *et al.* [8] found in step contraction tests conducted for a 5-s period that BB sEMG signals tended towards a more Gaussian distribution and a less linear distribution at 70% of MVC compared with 10%, 30%, 50% and 100% of MVC. Naik *et al.* [10] conducted step isometric MVC tests at 20%, 50%, and 80% of MVC for a 7–8-s period for flexor digitorum superficialis (FDS). They pointed out that the distribution of FDS sEMG signals tended to be more Gaussian as the force increased, but it also significantly tended towards a Gaussian process below 30% of MVC. Furthermore, Husssain *et al.* [11] showed that the distribution of right rectus femoris (RRF) sEMG signals was more Gaussian during slow to fast-walking trials. However, their linearity test results followed the reverse pattern of the Gaussianity test where the RRF signal became more linear in mid-paced walking trials and less linear in a fast-walking trial.

The majority of prior Gaussianity and linearity tests showed that sEMG signals exhibit a more Gaussian distribution as exertion increases. According to the physiological property of the sEMG signal, the central nervous system controls the generation of muscle force by regulating the number of active MUs (nMUs) and the firing rates (FRs) of MUs. As muscle forces increase, more and more MUs and FRs are activated [12]. Several experimental studies have preliminarily discussed that the distribution of sEMG signals is perhaps affected by nMUs [9,10,13]. In the present work, a hypothesis is proposed that non-Gaussianity and non-linearity levels for sEMG signals are associated with nMUs and FRs. Reviewing prior Gaussianity and linearity tests of sEMG signals, we found only experimental studies. It is worth noting that different experiments could yield distinct results. Nazrpour *et al.* [14] suggested that BB sEMG signals became a more "non-Gaussian distribution" below 25% of MVC, whereas Naik *et al.* [15] demonstrated that the distribution of FDS sEMG signals was a more "Gaussian distribution" below 30% of MVC. Possible factors that may lead to these discrepancies include electrode, cable and connector movement, muscle size, exertion level, and cross-talk (a signal contribution originating from other muscles). To limit experimental factors and investigate the change mechanism of the non-Gaussianity and non-linearity levels of sEMG signals in theory, we used a sEMG mathematical model to explore the present assumption. We found no simulated estimation for the non-Gaussianity and non-linearity levels of sEMG signals in the literature.

The purpose of this paper was to test the relationship between nMUs and non-Gaussianity levels for sEMG signals, and the relationship between nMUs and non-linearity levels of sEMG signals at three FRs. An sEMG signal model based on muscle system physiological characteristics was established to simulate nMUs at the three FRs. The HOS approach was used to test the non-Gaussianity and non-linearity levels of the simulated sEMG signals that were obtained from the sEMG simulation model. This study measured BB muscle activities; BB step contractions were performed at 10 levels from 10% to 100% of MVC in a 5-s period. The study initially provides a theoretical supports to quantitatively detect non-linearity and deviations from Gaussianity of the sEMG signal with the MU recruitment number and firing patterns underlying changes. Furthermore, the finding of this study has practical guiding significance for the assessment of muscle activity in the field of occupational medicine and has good potential application for improving prosthetic control in the field of rehabilitation engineering.

1 Simulation sEMG signal of biceps brachii

1.1 Physiological structure of BB

BB is the one of the most commonly used muscles. The sEMG of BB can reflect the muscle load and moving angle of the main joint of the individual, i.e., the shoulder and elbow. The study of BB has representative meaning. As mentioned before, most experiments have focused on BB muscle in discussing the non-Gaussianity and non-linearity levels of sEMG. We chose BB as the simulated model so that we could fully compare the theory and experiment research. The BB muscle is commonly described as a cylindrical volume conductor. It has a multiple-layer structure and an anisotropic media characteristic [16]. To develop a simulated model of the BB sEMG signal, the BB muscle structure and its parameters must be known (Figure 1). The artificial sEMG signals from BB muscle were hypothetically measured using a bipolar electrode. The interelectrode distance was 20 mm. BB structure input parameters are given in Table 1.

1.2 Intracellular action potential simulation

There are two sEMG models. The first model is based on the energy modulation of Gaussian noise, and can be used to analyze the global information of sEMG signals using the amplitude and power spectrum (PS). The second model is based on a physiological property, and can precisely describe MU anatomy [20]. In this paper, we used the second model. Intracellular action potential (IAP) was adopted as the starting point of this sEMG model. IAP is mathemati-

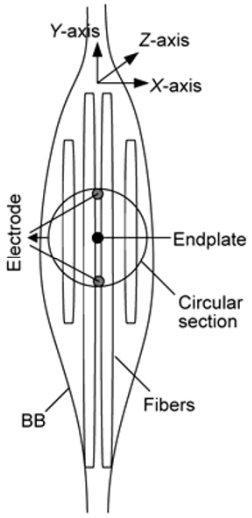

Figure 1 BB structure for the simulation sEMG model.

Table 1 BB structure parameters

Parameter	Values
Muscle area	Circular section
Thickness of the skin and fat Layer (hs+hf) [16]	4 mm
Fiber diameter (d) [17,18]	56 μm, SD=10 Range=±3 mm
Number of fibers in MU (nf)	800
Muscle radius [1]	45–55 mm
Muscle fibers density (ρ)	20 fibers mm^{-2}
MU size (D_{MU}) [19]	12 mm
Muscle fiber lengths $L_{0.5f}$ (right+left) [17]	70 mm, mean=0, SD=1, Range=±2 mm
Fiber-endplate position [18]	Mean=0, Range=±3 mm
Fiber-tendon distance [17]	Range=±6 mm
Fiber position [16]	Range ±1 MU radius
MU position [16]	Range ±1 muscle radius

cally formulated as [21]

$$e_i(z) = 768z^3e^{-z} - 90, \tag{1}$$

where $e_i(z)$ is fiber IAP; z is the axial direction (Figure 1) in millimeters; and i is an index identifying the MU.

1.3 Extracellular action potential simulation

The extracellular action potential (EAP) at an observation point [z_0, y_0] can be expressed as [22]

$$V_E(z_0, y_0) = K[\int_{S_1} \frac{\partial e(z)}{\partial z} \cdot \frac{1}{r} \mathrm{d}S + \int_S \mathrm{d}S \int_{-\infty}^{+\infty} \frac{\partial^2 e(z)}{\partial z^2} \cdot \frac{1}{r} \mathrm{d}z - \int_{S_2} \frac{\partial e(z)}{\partial (z)} \cdot \frac{1}{r} \mathrm{d}S, \tag{2}$$

where y is the radial direction (Figure 1) in millimeters; S_1 and S_2 are the fiber sections at the fiber ends; and r is the distance between the surface element dS and the observation point:

$$r = \sqrt{(z_0 - z)^2 + \sigma_z / \sigma_y y_0^2}. \tag{3}$$

Here anisotropy is introduced through σ_z and σ_y, which denote the axial and radial conductivity, respectively.

The part $I_m(z)$ corresponds to the transmembrane current of K'':

$$I_m(z) = K'' \cdot \frac{\partial^2 e(z)}{\partial z^2} = \frac{\pi d^2 \sigma_i}{4} \cdot \frac{\partial^2 e(z)}{\partial z^2}, \tag{4}$$

where σ_i is the intracellular conductivity.

1.4 Muscle fiber conduction velocity simulation

Nandedkar and Stålberg suggested that muscle fiber conduction velocity (MFCV) is related to fiber diameter [21]:

$$v = 2.2 + 0.05(d - 25), \tag{5}$$

where v is the conduction velocity in meters per second.

1.5 MU recruitment simulation

An MU is recruited when input excitation reaches its recruitment threshold. The assigned recruitment threshold excitation (*RTE*) in the MU pool follows an exponential rule in the form [19]

$$RTE(i) = \mathrm{e}^{\alpha \cdot i} = \mathrm{e}^{\frac{\ln(RR)}{n} \cdot i}, \tag{6}$$

where α is a coefficient used to establish the range of threshold values; and *RR* is the range of recruitment threshold values desired. This was set to be a broad MU recruitment range in this paper. That is, the last recruited MU recruitment threshold was set at 70% of the maximum excitation [23].

1.6 MU firing simulation

An MU's peaking firing rate (*PFR*) is inversely proportional to the recruitment threshold according to [19]

$$PFR(i) = PFR(1) - PFRD \cdot \frac{RTE(i)}{RTE(120)}, \ i = 2:120, \tag{7}$$

where $PFR(1)$ is the assigned *PFR* of the first recruited unit; *PFRD* is the desired difference of the PFR between the first and the last units recruited; $RTE(i)$ is the recruitment threshold of the studied MU; and $RTE(120)$ is the recruitment threshold of the last recruited MU. The MU discharges at a minimum FR of 8 Hz when the excitatory drive reaches its recruitment threshold. Three FRs were simulated [23]. For FR1, the slope of the excitatory drive-FR relation for an MU increased with increasing recruitment threshold. For FR2, the slope of the excitatory drive-FR relation was set

the same for all MUs, whereas *PFR* was linked to the mechanical properties of MUs. For FR3, the slope of the excitatory drive-FR relation was set the same for all MUs. *PFR* of a MU was inversely proportional to its recruitment threshold.

1.7 Muscle force generation model

Muscle force was modeled as an exponential form, linked to the recruitment threshold and varying over a wide range [19]:

$$F(i) = e^{\mu \cdot i} = e^{\frac{\ln(RF)}{n} i}, \quad (8)$$

where $F(i)$ is the force; μ is a coefficient used to establish a range of twitch force values; and RF is the desired range of twitch force values, which is set to 100. The step force was simulated as 10%, 20%, 30%, 40%, 50%, 60%, 70%, 80%, 90%, and 100% of MVC.

An sEMG signal simulator was established according to muscle physiological features and the electrode configuration. It is equivalent to the accumulation of 120 MUAPs. Table 2 lists the pertinent parameters from sections 1.2 to 1.7.

Table 2 MUAP parameters of the simulated sEMG signal

Parameter	Values
Sample rate	1024 Hz
Muscle contraction period	5 s
Maximum nMUs [17]	120
Firing rates [23]	FR1, FR2, FR3
Recruitment threshold [12]	70% of maximum excitation
MFCV	3.19 m s^{-1}
Minimum FR [12]	8 Hz
Axial conductivity (σ_z) [17]	0.5 s m^{-1}
Radial conductivity (σ_y) [17]	0.1 s m^{-1}
Intracellular conductivity (σ_i) [24]	1.01 s m^{-1}

2 Gaussianity test and linearity test

To perform a bispectrum analysis of HOS, the artificial sEMG signals $x(n)$ were first divided into a series of epochs adjusted to a zero mean value to exclude any signal offset arising from electrode half-cell potentials [25]. The bispectrum analysis is defined as a Fourier transform of the third-order cumulant sequence:

$$B(f_1, f_2) = E[X(f_1)X(f_2)X^*(f_3 = f_1 \pm f_2)], \quad (9)$$

where $X(f)$ is the Fourier transform of time traces of $x(n)$; $E[\cdot]$ is the ensemble expectation; and f_i (i=1, 2, 3) is the wave frequency. There is phase coupling because of non-linear interactions between harmonic components when $k_1 \pm k_2 = k_3$ and $f_1 \pm f_2 = f_3$, with ki being the wave number.

To quantify the non-Gaussianity level of a random process, the normalized bispectrum is defined as

$$B_{\text{norm}}(f_1, f_2) = \frac{E[X(f_1)\mathrm{X}(f_2)\mathrm{X}^*(f_1 \pm f_2)]}{\sqrt{P(f_1)P(f_2)P(f_1 \pm f_2)}}, \quad (10)$$

where $P(f)$ is the PS.

Consequently, the Gaussianity test is given by

$$S_{\text{g}} = \sum \left| B_{\text{norm}}(f_1, f_2) \right|^2, \quad (11)$$

where S_{g} involves deciding whether the estimated bicoherence is zero. A non-Gaussianity assumption was accepted when the probability of a false alarm (Pfa) is less than 5% [8]. Linearity test S_ℓ involves deciding whether the estimated bicoherence is constant in the bi-frequency domain, employing the absolute difference (dR) between a theoretical (R') and an estimated inter-quartile range (R). A non-linearity hypothesis was adopted when $\mathrm{d}R/R' > 2$ [8].

3 Time-domain and frequency-domain analysis

The time and frequency domains both fail to consider the non-Gaussianity and non-linearity levels for sEMG signals, and ignore sEMG phase information. However, these two conventional techniques are highly reliable estimators of exertion variation. The root mean square (RMS) from the time domain and the median frequency (MDF) from the frequency domain were also used to characterize BB muscle activities [26]. RMS is defined as

$$RMS = \sqrt{\frac{1}{N}\sum_{j=1}^{N} x_j^2}, \quad (12)$$

where x_j is the jth sample of a signal; and N is the number of samples in the epoch.

MDF is computed using a 512-point Hanning window:

$$\int_0^{f_{\text{med}}} P(f)\mathrm{d}f = \frac{1}{2}\int_0^{f_s/2} P(f)\mathrm{d}f, \quad (13)$$

where f_{med} is the MDF; and f_s is the sampling frequency.

4 Results

4.1 sEMG simulation results

Figure 2 illustrates the artificial BB sEMG signals from 10% to 100% of MVC for the three FRs. To conveniently compare the amplitudes of sEMG signals, the signals are shown in normalized form. The blue long-dash lines, red-solid lines, and green short-dash lines present sEMG signals for FR1, FR2 and FR3, respectively. The sEMG signal amplitudes of the three FRs evidently broadened from 10% to 100% of MVC.

4.2 Gaussianity test and linearity test results

Figure 3 shows the Pfa values and S_g values of the Gaussianity test, and the S_ℓ values of the linearity test for the three FRs. The horizontal ordinate in Figure 3 reflects that nMUs increased as the MVC level increased. For the three FRs, the sEMG signals for nMUs were 65, 84, 96, 104, 110, 115, 120, 120, 120 and 120 corresponding to the 10 levels of MVC. Viewing the curves in Figure 3, most Pfa values were less than 5%. Several Pfa values were more than 5% and

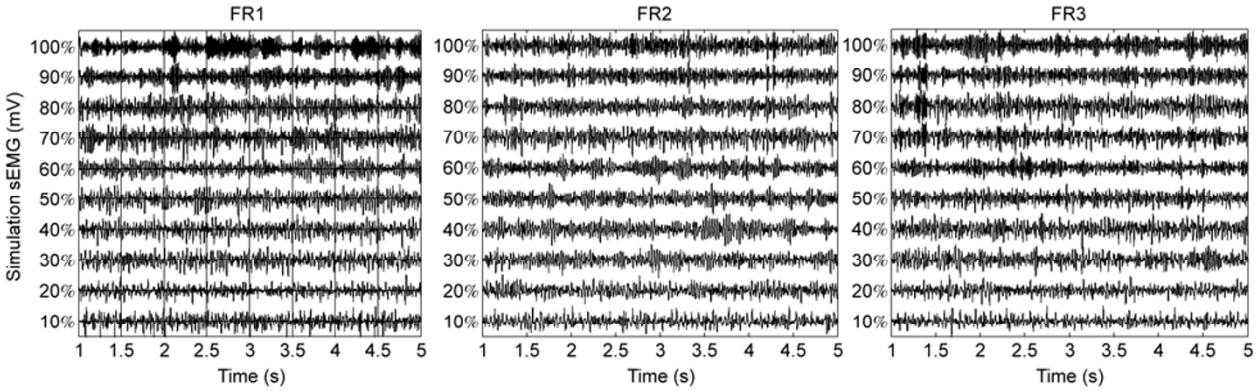

Figure 2 sEMG signals from 10% to 100% of MVC for the three FRs.

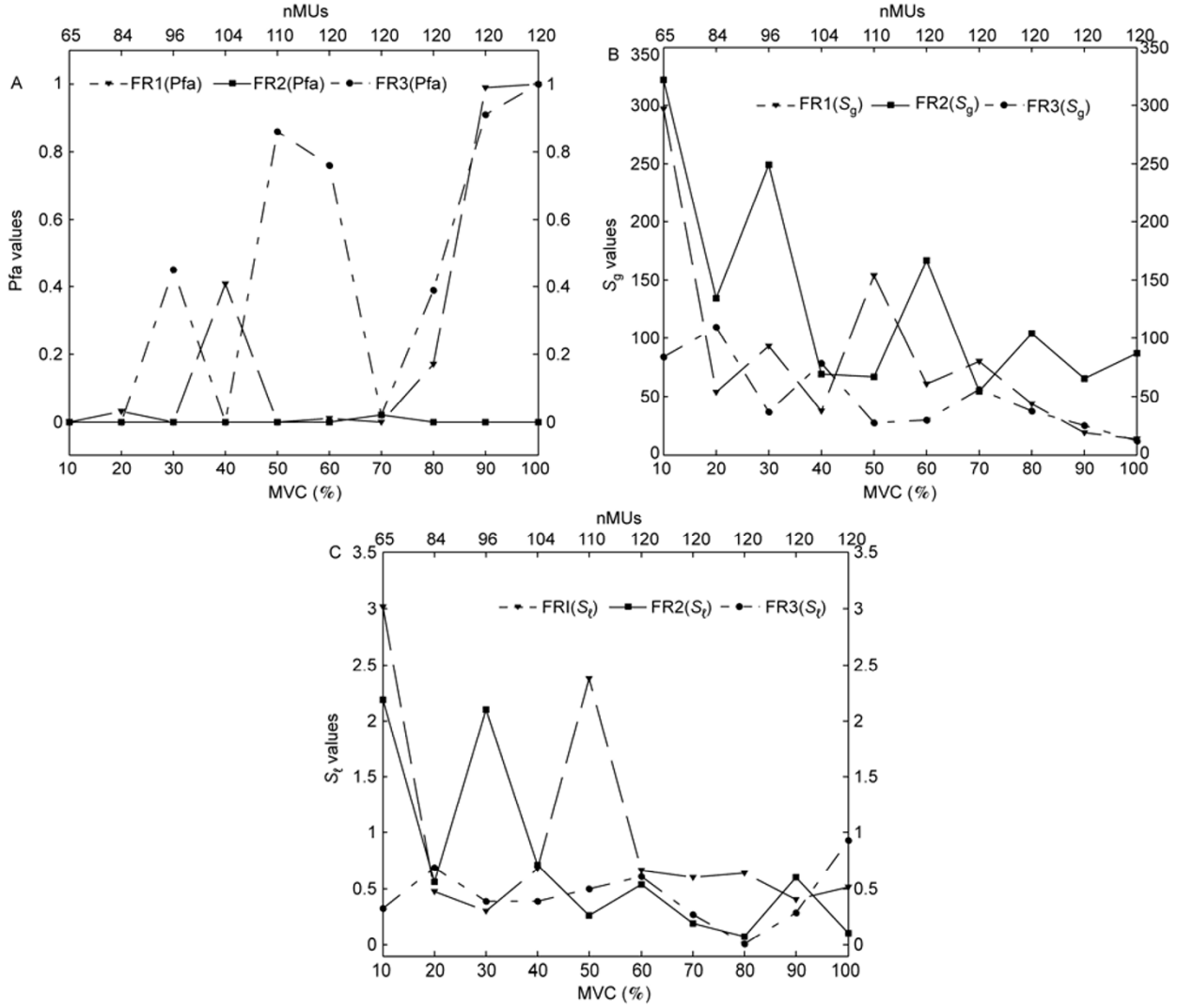

Figure 3 Gaussianity and linearity tests for the three FRs. A, Pfa values of the Gaussianity test. B, S_g values of the Gaussianity test. C, S_t values of the linearity test.

were approximately 1 (Table 3). Most dR/R' values were smaller than 2. The dR/R' values that are much larger than 2 are listed in Table 4. As MVC levels and nMUs increased, the S_g and S_ℓ results of sEMG signals for the three FRs all declined sharply.

4.3 Multivariate analysis of covariance test results

A multivariate analysis of covariance (MANOVA) was conducted to test the effects of nMUs and FRs on the non-Gaussianity and non-linearity levels of the sEMG signal. In Table 5, df is the number of degrees of freedom; F is the F-statistics; and P is the P-value probability. The dependent variables are S_g and S_ℓ, and the independent variables are nMUs and the FR. nMUs and the FR significantly affected S_g and S_ℓ at the P=0.000 level. Interaction between nMUs and the FR also affected the S_g and S_ℓ at the P=0.003 and P=0.000 levels, respectively. MANOVA gives four results: (i) there were differences in the Gaussianity and linearity test results for the sEMG signal because of the change in the FR when nMUs was held constant; (ii) there were differences in the sEMG signal Gaussianity and linearity test results because of the change in nMUs when the FR was held constant; (iii) the interactive relationship between nMUs and the FR affected the Gaussianity and linearity test results for the sEMG signal; and (iv) the FR, nMUs, the interactive effects between the FR and nMUs, and test errors were the significant predictor, could explain 97.1% and 99.3% of the total variance of Gaussianity test results and linearity test results, respectively (see footnotes a and b in Table 5).

Table 3 Gaussianity test Pfa values that are approximately 1

Strategies	MVC	Pfa values
FR1	90%	0.99
	100%	1.00
FR3	50%	0.86
	60%	0.76
	90%	0.91
	100%	1.00

Table 4 Linearity test dR/R' values that are more than 2

Strategies	MVC	dR/R' values
FR1	10%	3.01
	50%	2.38
FR2	10%	2.19
	30%	2.1

Table 5 MANOVA test results for the three FRs

Source	Dependent variables	df	F	P
Corrected model	S_g [a)]	20	14.90	0.000
	S_ℓ [b)]	20	60.40	0.000
nMUs	S_g	6	25.14	0.000
	S_ℓ	6	104.10	0.000
FRs	S_g	2	32.32	0.000
	S_ℓ	2	72.29	0.000
nMUs *FRs	S_g	12	7.41	0.003
	S_ℓ	12	40.47	0.000

a) R^2=0.971 (adjusted R^2=0.906). b) R^2=0.993 (adjusted R^2=0.976).

4.4 Bivariate correlation test results

A bivariate correlation test was carried out to determine the correlation between nMUs and S_g, and the correlation between nMUs and S_ℓ for the three FRs. The Pearson correlation coefficients in Table 6 indicate that the nMUs-S_g relationship and the nMUs-S_ℓ relationship both have negative correlation. In addition, the S_g-S_ℓ relationship has positive correlation. The highest correlation (r=–0.83) was between nMUs and S_ℓ for FR2 (P<0.01). All Pearson coefficients for FR1 and FR2 were clearly significant (P<0.05). The correlation coefficients for the nMUs-S_ℓ relation and those for the S_g-S_ℓ relation for FR3 were very low (see footnotes * and ** in Table 6).

4.5 Time-domain and frequency-domain results

RMS and MDF results of the simulated sEMG signals for the three FRs are summarized in Figure 4. RMS increased markedly as the force and nMUs increased. MDF results did not shifted to the lower frequencies with muscle force and nMUs gradually increasing. In contrast, MDF results for the three FRs slightly shifted to the higher frequencies for all levels of exertion.

5 Discussion

The purpose of this study was to test the hypothesis that the non-Gaussianity and non-linearity levels of sEMG signals are associated with nMUs at three FRs. Prior experimental studies concluded that the non-Gaussianity and non-linearity levels of sEMG signals change with muscle force levels. However, the change mechanism of sEMG non-Gaussianity and non-linearity levels for the nMUs and FR strategies of

Table 6 Bivariate correlation test results for the three FRs[a)]

Parameters	nMUs	FR1 (S_g)	FR2 (S_g)	FR3 (S_g)
nMUs	1			
FR1 (S_g)	–0.74*	1		
FR2 (S_g)	–0.79**		1	
FR3 (S_g)	–0.73*			1
FR1 (S_ℓ)	–0.69*	0.96**		
FR2 (S_ℓ)	–0.83**		0.93**	
FR3 (S_ℓ)	–0.40			0.49

a) *, P<0.05; **, P<0.01.

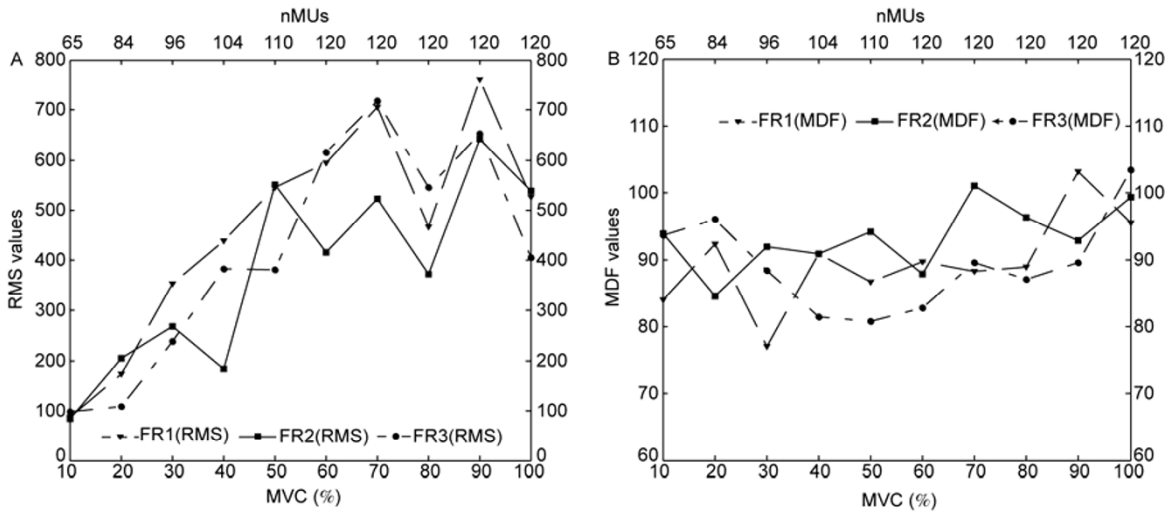

Figure 4 Time-domain and frequency-domain results for the three FRs. A, RMS values of time-domain analysis. B, MDF values of frequency-domain analysis.

muscle is not directly available from experimental studies, and remains elusive. Thus, we used a mathematical simulated model to investigate the present hypothesis in theory. This study quantitatively shed light on the relation between nMUs and the non-Gaussianity levels of sEMG signals, and the relation between nMUs and the non-linearity levels of the sEMG signal for the three FRs. The current effort may stimulate further work on two fronts. First, it can be used to objectively and comprehensively evaluate muscle capability in a normal individual and an individual suffering from a neuromuscular disorder. Second, it can be applied in the control of prosthetics for an individual with an amputation or congenitally deficient limb. The mathematical simulated model can avoid the effects of real physical world factors, such as electrode movement and cross-talk. It was developed according to musculoskeletal system physiology characteristics. The model deduced sEMG signals involving spatial (active MUs) and temporal (FR) information. The levels of the non-Gaussianity and non-linearity of simulated sEMG signals were estimated using the HOS approach. A MANOVA and a bivariate correlation test were used to quantify the test results for the nMUs-Gaussianity relationship, the nMUs-linearity relationship, and the Gaussianity-linearity relationship. The study contributes three major findings.

First, the horizontal ordinate in Figure 3 shows that the nMUs for the three FRs had the same incremental trend as exertion increased. The BB sEMG signals for all three FRs achieved full MU recruitment at 70% MVC. From eq. (6), we know that nMUs depend on the exertion level and *RR*, and are independent of the FR strategy. The FR does not affect nMUs at each exertion level. All MUs were recruited at 70% of MVC because the MU recruitment range was set at 70% maximum excitation.

Second, Figure 3 shows that S_g and S_ℓ significantly decrease as forces and nMUs increase. S_g is estimated in a χ^2 distribution test. The principle of the χ^2 distribution test is

$$\chi^2 = \sum \frac{(f_0 - f_e)^2}{f_e}, \tag{14}$$

where f_0 is the observed frequency; and f_e is the theoretical frequency. For a smaller value of S_g, there is little difference between f_0 and f_e. In this paper, f_0 is the frequency distribution of the sEMG signals; and f_e is the theoretical Gaussian frequency distribution. It is clear that nMUs increased and S_g decreased as the force increased for all three FRs. Thus, the Gaussianity test revealed that sEMG signals tended toward a more Gaussian distribution as the force and nMUs increased at all three FRs. The non-Gaussianity of sEMG signals below 40% MVC was significant for all three FRs.

The linearity of sEMG signals was calculated as $|R'-R|$. Here, R' corresponds to $\chi_2^2(\lambda)$, that is, a χ^2 distributed random variable having two degrees of freedom and a non-centrality parameter. R is derived from the estimated squared bicoherence. In Figure 3C, nMUs increased and dR decreased as the force increased at all three FRs. The linearity test of sEMG signals revealed that sEMG signals were a more linear distribution as the force increased at all three FRs. Additionally, the linearity of sEMG signals above 60% of MVC was significant at all three FRs.

In Table 3, the Pfa values for FR1 at 90% and 100% of MVC, and for FR3 at 50%, 60%, 90%, and 100% of MVC were approximately 1. We accepted the Gaussian hypothesis at these MVC levels. In Table 4, the dR/R' values for FR1 at 10% and 50% of MVC, and for FR2 at 10% and 30% of MVC were more than 2. We accepted the non-linear hypothesis at these MVC levels. Furthermore, all Pfa values for FR2 were less than 5%, and all dR/R' values for FR3 were less than 2. In virtue of the indeterminable nature and

complexity of human muscle activities, and the unknown precise motoneuron FR distribution for different MUs, we speculate that the non-Gaussianity and non-linearity discrepancy among the three FRs was caused by different *PFR* values for the three FRs (eq. (7)). For FR1, all MUs finally reached the same *PFR* at 70% of MVC (Figure 5A). In the FR2 simulation, the *PFR* values were linked to the mechanical properties of MUs. That is, later-recruited large rapidly contracting units were assigned higher *PFR*s than were those with lower recruitment thresholds and with small twitches and slow contraction times (Figure 5B). In FR3 simulation, slope of the excitatory drive-FR relation was set to be the same for all MUs. The *PFR* of an MU was inversely proportional to its recruitment threshold (Figure 5C) [23]. The three-FR waveforms altered the sEMG signal distribution.

Finally, the correlation between nMUs and non-Gaussianity, and the correlation between nMUs and the non-linearity, were quantitatively analyzed at the three FRs. The MANOVA test and bivariate correlation test were performed to shed light on our hypothesis (see results in Tables 5 and 6). The MANOVA test validated that not only the two main factors nMUs and the FR but also interaction between these factors was responsible for the changes in the non-Gaussianity and non-linearity levels of sEMG signals. The bivariate correlation test demonstrated that nMUs was negatively correlated to both the Gaussianity and linearity results of sEMG signals. Furthermore, for all three FRs, the Gaussianity test results of sEMG signals was positively correlated to the linearity test results.

Similarly, Bilodeau *et al*. [5] and Kaplanis *et al.* [8] both reported that BB sEMG signals tended to be a more Gaussian distribution as exertion increased. Nazarpour *et al.* [9] found that the non-Gaussianity of BB sEMG signals below 25% of MVC was significant. Naik *et al.* [10] found that FDS sEMG signals tended towards a Gaussian distribution as exertion increased. However, they also pointed out that FDS sEMG signals tended to be a more Gaussian distribution below 30% of MVC. The later finding of Naik is the converse of our result. The discrepancy may stem from the difference in MU recruitment between small and large muscles. Small muscles have been reported to have narrow MU recruitment, such as in the case of FDS. Large muscles have a mixed fiber composition. They are generally regarded as having a broad MU recruitment range, such as the case for BB [23]. Although the FR and MU recruitment both contribute to force production, the FR plays a more important role in small muscles and MU recruitment is important in large muscles [27]. Small muscle MUs obey the so-called "size principle" [28], which states that MUs are activated in order from the smallest to the largest MU. This "size principle" does not explain the behavior of large muscles. Thus, we argue that the MU recruitment range and "size principle" explain the difference between small and large muscles.

The sEMG linearity test carried out by Kaplanis *et al.* [8] revealed that BB sEMG signals exhibited more Gaussianity at 70% of MVC, while sEMG signals showed less linearity at 70% of MVC. A more recent study by Hussian *et al.* [11] performed sEMG signal linearity tests for the RRF. They reported that the linearity test followed the reverse pattern of the Gaussianity test. Unlike these linearity results, our linearity test results were positively correlated to the Gaussianity results. We tentatively argue that this apparent conflict results from muscle fatigue. In time and frequency domains, if the EMG amplitude increases and the EMG spectrum shifts to the right (i.e., the time-domain and frequency-domain curves turn upward), then the probable cause is an increase in muscle force. If the EMG amplitude increases and the EMG spectrum shifts to the left (i.e., the time-domain curve turns upward and the frequency-domain curve turns downward), then this is considered to be a result of muscle fatigue [14]. The results in the time and frequency domains for the three FRs are shown in Figure 4. The sEMG signal RMS values increased, and simultaneously the MDF values slightly shifted to the higher frequencies. Thus, our sEMG signal variation is related to the force. Time-domain and frequency-domain analyses were carried out

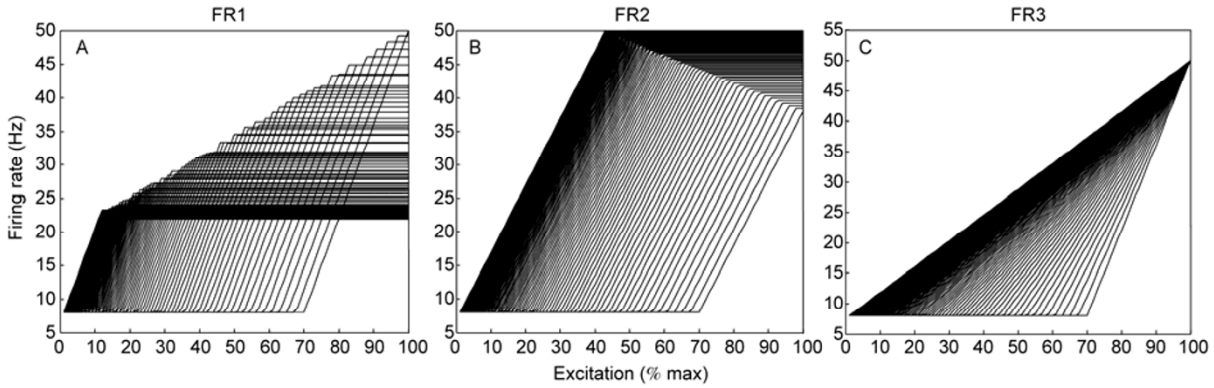

Figure 5 BB broad recruitment simulation for the three FRs.

by Kaplanis *et al.* and Hussian *et al.*, who found that the time-domain outputs increased and the frequency-domain outputs shifted to the lower frequencies as force level increased. The sEMG signal variations of those two studies were described as fatigue-induced. We deduce that sEMG signals have a more Gaussian and more linear distribution in the bi-frequency domain probably because of an increase in large muscle force, and they have a more Gaussian and less linear distribution probably because of large muscle fatigue.

6 Conclusion

The simulated sEMG signal model in the present research was used to quantitatively test the relation between nMUs and the non-Gaussianity levels of sEMG signals, and the relation between nMUs and non-linearity levels of the sEMG signal for three FRs. Results showed that the BB sEMG signal was a more Gaussian and more linear distribution as nMUs and exertion increased. The non-Gaussianity level of the sEMG signal below 40% MVC is significant, and the linearity level of the sEMG signal above 60% MVC is significant. The changes in non-Gaussianity and non-linearity levels of the sEMG signal essentially rely on nMUs and FRs.

This work was supported by the National High Technology Research and Development Program of China and the National Basic Research Program of China (Grant No. 2011CB7000).

Abbreviations

Biceps Brachii	BB
Extracellular Action Potential	EAP
Firing Rate	FR
Flexor Digitorum Superficialis	FDS
Higher-order Statistics	HOS
Intracellular Action Potential	IAP
Motor unit	MU
Median Frequency	MDF
Maximum Excitation	ME
Motor Unit Action Potential	MUAP
Maximum Voluntary Contraction	MVC
Muscle Fiber Conduction Velocity	MFCV
Multivariate Analysis of Covariance	MANOVA
Number of active MUs	nMUs
Peaking Firing Rate	PFR
Power Spectrum	PS
Probability of False Alarm	Pfa
Right Rectus Femoris	RRF
Root Mean Square	RMS
Recruitment Threshold Excitation	RTE
Surface electromyography	sEMG
Gaussianity test	S_g
Linearity test	S_ℓ

1 Buchthal F, Erminio F, Rosenfalck P. Motor unit territory in different human muscles. Acta Physiol Scand, 1959, 45: 72–87
2 Merletti R, Rainoldi A, Farina D. Electromyography: Physiology, Engineering and Noninvasive Application. New Jersey: John Wiley & Sons, 2004
3 Merletti R, Roy S H, Kupa E, *et al*. Modeling of surface myoelectric signals—Part II: model-based signal interpretation. IEEE Trans Biomed Eng, 1999, 46: 821–829
4 Day S J, Hulliger M. Experimental simulation of cat electromyogram: evidence for algebraic summation of motor-unit action-potential trains. J Neurophysiol, 2001, 86: 2144–2158
5 Bilodeau M, Cincera M, Arsenault A B, *et al*. Normality and stationarity of EMG signals of elbow flexor muscles during ramp and step isometric contractions. J Electromyogr Kines, 1997, 7: 87–96
6 Zazula D. Experience with surface EMG decomposition using higher-order cumulants. In Proceedings of Signal Processing 2001 of IEEE Workshop, Poznãn, Poland, 2001. 19–24
7 Shahid S, Walker J, Lyons G M, *et al*. Application of higher order statistics techniques to EMG signals to characterize the motor unit action potential. IEEE Trans Biomed Eng, 2005, 52: 1195–1209
8 Kaplanis P A, Pattichis C S, Hadjileontiadis L J, *et al*. Surface EMG analysis on normal subjects based on isometric voluntary contraction. J Electromyogr Kines, 2009, 19: 157–171
9 Nazarpour K, Sharafat A R, Firoozabadi S M P. Application of higher order statistics to surface electromyogram signal classification. IEEE Trans Biomed Eng, 2007, 54: 1762–1769
10 Naik G, kumar D. Evaluation of higher order statistics parametes for multi channel sEMG using different force levels. In: 33rd Annual International Conference of the IEEE, Boston, USA, 2011. 3869–3872
11 Hussain M S, Mamun M D. Effectiveness of the wavelet transform on the surface EMG to understand the muscle fatigue during walk. Meas Sci Rev, 2012, 12: 28–33
12 Zhou P, Rymer W Z. Can standard surface EMG processing parameters be used to estimate motor unit global firing rate? J Neural Eng, 2004, 1: 99–110
13 Kernell D. Organized variability in the neuromuscular system: a survey of task-related adaptations. Arch Ital Biol, 1992, 130: 19–66
14 Staudenmann D, Roeleveld K, Stegeman D F, *et al*. Methodological aspects of sEMG recordings for force estimation-A tutorial and review. J Electromyogr Kines, 2009, 20: 375–387
15 Turker K S, Miles T S. Cross-talk from other muscles can contaminate EMG signals in reflex studies of the human leg. Neurosci Lett, 1990, 111: 164–169
16 Wang W, Stefano A D, Allen R. A simulation model of the surface EMG signal for analysis of muscle activity during the gait cycle. Comput Biol Med, 2006, 36: 601–618
17 Gabriel D A, Kamen G. Experimental and modeling investigation of spectral compression of biceps brachii SEMG activity with increasing force levels. J Electromyogr Kines, 2009, 19: 437–448
18 Duchêne J, Hogrel J Y. A model of EMG generation. IEEE Trans Biomed Eng, 2000, 47: 192–201
19 Fuglevand A J, Winter D A, Patla A E. Models of recuitment and rate coding organization in motor-unit pools. J Neurophysiol, 1993, 70: 2470–2488
20 McGill K C. Surface electromyogram signal modelling. Med Biol Eng Comput, 2004, 42: 446–454
21 Nandedkar S D, Stålberg E. Simulation of sigle fiber action potentials. Med Biol Eng Comput, 1983, 21: 158–165
22 LorentedeNó R. Analysis of the distribution of action currents of nerve in volume conductors. Stud Rockfeller Inst Med Res, 1974, 132: 384–477

23 Zhou P, Rymer W Z. Factor governing the form of the relation between muscle force and the EMG: A simulation study. J Neurophysiol, 2004, 92: 2878–2886
24 Andreassen S, Rosenfalck A. Relation of intracellular and extracellular action potentials of skeletal muscle fibers. OCR Crit Rev Biomed Eng, 1981, 6: 267–306
25 Sigl J C, Chamoun N C. An introduction to bispectral analysis for the electroencephalogram. J Clin Monit, 1994, 10: 392–404
26 Zhou Q X, Chen Y H, Ma C, *et al*. Evaluation of upper limb muscle fatigue based on surface electromyography. Sci China Tech Sci, 2011, 54: 939–944
27 DeLuca C J, LeFever R S, McCue M P, *et al*. Behaviour of human motor units in different muscles during linearly varying contractions J Physiol, 1982, 329: 113–128
28 Henneman E. Relation between size of neurons and their susceptibility to discharge. Science, 1957, 126: 1345–1347